

EVALUATION OF FRACTURE TOUGHNESS OF X-60 PIPELINE STEEL IN-SITU HIGH-PRESSURE HYDROGEN GAS

^{1,2}Jan KANDER, ¹Petr ČÍŽEK, ¹Gabriela ROŽNOVSKÁ, ^{1,2}Petr JONŠTA

¹ MATERIÁLOVÝ A METALURGICKÝ VÝZKUM, Ostrava, Czech Republic, EU, jan.kander@mmvyzkum.cz
² VSB - Technical University of Ostrava, Ostrava, Czech Republic, EU

https://doi.org/10.37904/metal.2025.5120

Abstract

The European Union is committed to replacing natural gas with hydrogen by 2050 as part of its search for clean and sustainable energy sources. Given these goals, it is crucial to examine the materials used in current gas infrastructure and assess their susceptibility to hydrogen embrittlement, a common form of material degradation induced by hydrogen. In this article, a comparative evaluation of fracture toughness was assessed on CT specimen from operated X-60 steel used in Czech gas distribution infrastructure. J-R curves in air and in-situ 10 MPa hydrogen gas were constructed and initiation value $J_{0.2}$ was determined, followed by SEM fractographic analysis of fracture surfaces. The results showed significant decrease in initiation value $J_{0.2}$ in high-pressure hydrogen, which was accompanied by fracture morphology change in stable growth region from ductile dimple with micro void coalescence to quasi-cleavage/cleavage.

Keywords: Fracture toughness, J-R curve, high-pressure hydrogen, X-60 steel

1. INTRODUCTION

With regard to the socially relevant topic of decarbonization and achieving so-called carbon neutrality related to the Green Deal agreement, but also to the REPowerEU project, which seeks to ensure sustainable energy sources for Europe and eliminate dependence on Russian energy sources (gas, oil) [1], the gas industry is also becoming an area of current interest, where the carbon footprint should be reduced by adding hydrogen (over time to full replacement) to natural gas. As part of the Green Deal agreement and the European Hydrogen Backbone (EHB) initiative, a backbone hydrogen distribution network for the whole of Europe should be built by 2050, where the use and minor modifications of the existing gas infrastructure are expected, which should lead to significant material savings, because the costs of operating the existing network are about 20% compared to building a new network [2-5].

In recent years, hydrogen has been increasingly discussed as a source of ecological fuel and energy. The basis of this energy transformation lies in the first phase in the addition of hydrogen to natural gas and thus in the reduction of CO_2 emissions. The next phase is to gradually increase the hydrogen content in the gas infrastructure to 50 % by 2050, while medium to long-term scenarios include full substitution of natural gas by pure hydrogen. The basic problem of this transitional phase is the minimum information on the current state of the gas infrastructure and the degrading effect of hydrogen on the steel pipes currently used in the gas network.

Most local pipeline distribution systems contain at least a polyethylene liner (or are completely plastic), which should be much more resistant to the effects of hydrogen, together with much lower operating parameters of local networks compared to backbone networks. However, the problem arises with backbone networks, where the pipes are made of steel and operate at significantly higher pressures and flows; according to available information, backbone routes in the Czech Republic constitute approximately 40-45 % of the entire gas infrastructure [6].



2. EXPERIMENTAL MATERIAL AND METHODS

The main aim of the experimental work was to construct and compare J-R curves in air and high-pressure hydrogen. Experimental material was X-60 operated pipeline (diameter 1200 mm) which is a commonly used steel in Czech gas infrastructure, chemical composition analysed by combustion analysis (C, S) and XRF (other) is in **Table 1**.

Table 1 Chemical composition of the X-60 pipeline (weight %)

Element	С	S	Mn	Si	Р	Cu	Ni
X-60 pipeline	0.130	0.010	1.70	0.47	0.017	0.025	0.019

Table 1: continued

Element	Cr	Мо	V	Ti	Nb	W	Со
X-60 pipeline	0.028	0.009	0.099	<0.005	0.046	<0.005	0.003

The measurements and calculations for the J-R curve evaluation were carried out according to the ČSN ISO 12135 standard [7]. For the determination of the $J_{0.2}$ initiation value, 10 C(T) specimens were prepared with a thickness B = 12.5 mm, and a width W = 25 mm. Initial fatigue cracks were cycled into all test specimens on an MTS 100 kN servo hydraulic testing machine to give a maximum stress intensity factor of around 30 MPa·m^{1/2}. Five specimens were tested in air and other five in autoclave in 10 MPa hydrogen gas. The tests in air were carried out according to ISO 12135, the crossbar speed was chosen so that the rate of increase of the stress intensity factor dK/dT was about 0.6 MPa·m^{1/2}/s in the linear region of the loading diagram. During the test, the crack tip opening (CTOD) was measured with a clamp-on sensor.

For the high-pressure hydrogen testing, a 0.5 I autoclave was embedded into the MTS 100 kN servo hydraulic testing machine, **Figure 1**.



Figure 1 Autoclave built-in testing machine, CT specimen in jaws

After clamping the sample in the jaws of the machine, the autoclave was first flushed with nitrogen and then vacuumed. It was then progressively pressurized with hydrogen up to a working pressure of 10 MPa (100 bar). Once the pressure was reached, the actual test began by slightly loading the specimen to break the oxide film on the crack surface and unloading. The crossbar speed corresponded to the rate of increase of the stress



intensity factor change dK/dt of maximum 0.014 MPa.m $^{1/2}$ /s. Due to the confined and limited space in the autoclave, a clamp-on sensor could not be used for the high-pressure hydrogen test. Instead, the notch opening was measured before and after the test and difference between the two values was recorded as V_{pl} . The test data are summarized in **Table 2**. The constructed J-R curves are compared graphically in **Figure 2**.

Table 2 Data and parameters for the fracture toughness evaluation

Sample	Environment	Presssure (MPa)	a ₀ (mm)	Δa (mm)	V _{pl} (mm)	F (N)	CTOD (mm)	J ₀ (N·mm ⁻¹)	J _{0.2} (N·mm ⁻¹)
X60-1	air	atm.	14.37	0.94	-	13 528	0.148	182.0	
X60-2	air	atm.	12.82	0.81	-	17 461	0.151	185.3	
X60-3	air	atm.	14.09	0.31	-	14 455	0.104	127.1	84.87
X60-4	air	atm.	13.25	0.53	-	16 377	0.087	107.3	
X60-5	air	atm.	13.91	0.14	-	14 918	0.056	68.2	
X60-6	H ₂ , 10 MPa	10	14.90	0.51	0.07	9 350	0.027	33.0	
X60-7	H ₂ , 10 MPa	10	14.30	1.14	0.08	9 621	0.028	34.5	
X60-10	H ₂ , 10 MPa	10	13.29	0.25	0.00	11 138	0.013	15.7	16.23
X60-8	H ₂ , 10 MPa	10	14.13	0	0.02	8 319	0.013	15.9	
X60-9	H ₂ , 10 MPa	10	13.45	0	0.00	8 202	0.007	8.9	

Where:

 a_0 = length of the initial fatigue crack (mm)

Δa = length of the stable crack growth increment

V_{pl} = notch mouth opening (mm)

F = force after unloading (N)

CTOD = crack tip opening displacement (mm)

J₀ = calculated J-integral value

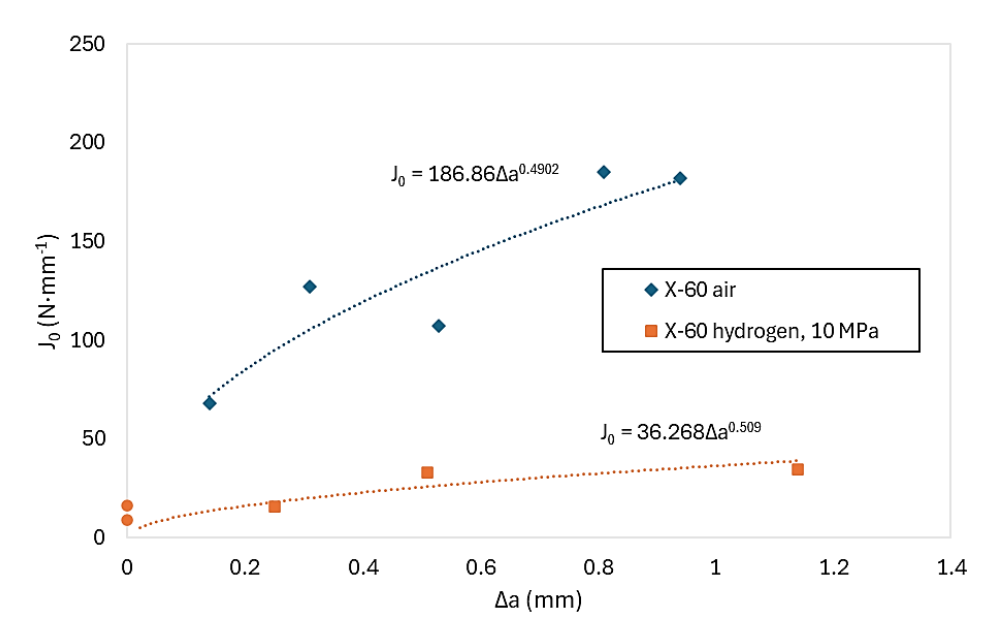


Figure 2 Comparison of the J-R curves in different environments



After reaching the selected notch opening for each specimen, the test was terminated, the specimen was unloaded, the hydrogen was drained from the autoclave and the autoclave was flushed again with nitrogen. The test specimen, removed from the jaws of the testing machine, was heated to approximately 300 °C to contrast the initial crack and stable increment region and then broken in liquid nitrogen. The lengths of the initial cracks and their increments were measured on a measuring microscope and then the samples were subjected to fractographic analysis by SEM.

Stable crack growth increment in air-loaded specimens was exclusively consisted of a transcrystalline ductile dimple fracture mechanism, **Figure 3**. Cracks occurred abundantly on all test specimens, both in the initial region of the pre-cycled fatigue crack, **Figure 4a**), and in the region of stable growth, where they appeared to be coarser, **Figure 4b**).

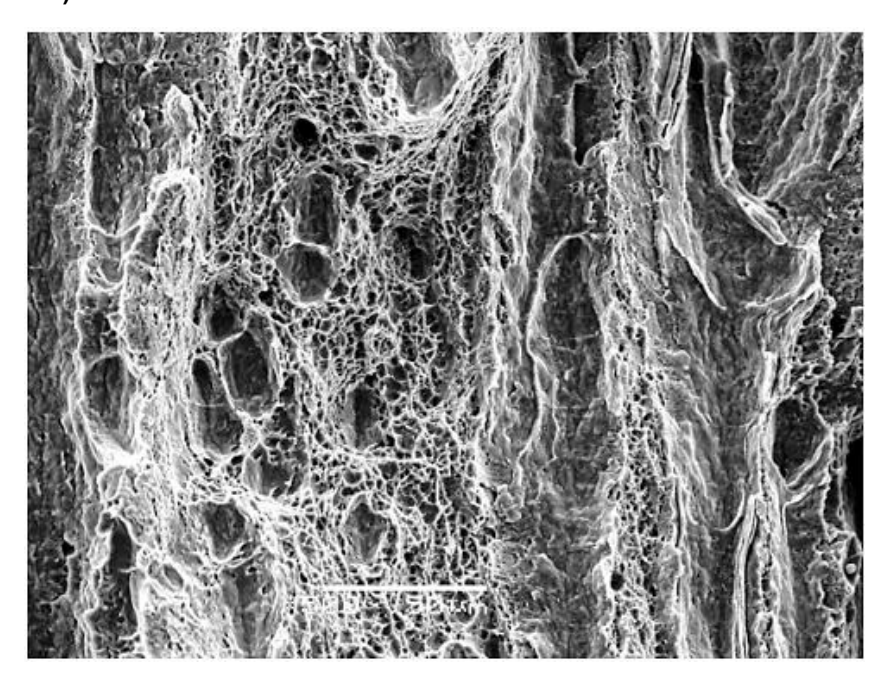


Figure 3 Stable crack growth increment created by transcrystalline ductile dimple fracture in air-loaded specimen

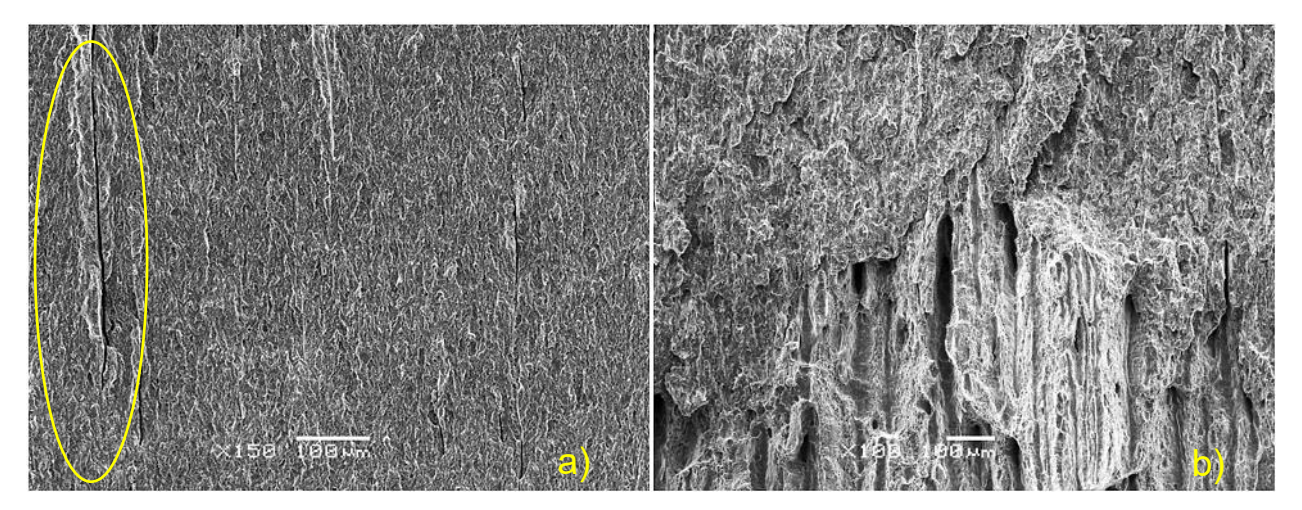


Figure 4a) Cracks in the initial region of the pre-cycled fatigue crack **4b)** cracks in the stable crack growth region



Stable crack growth increment was observed on three out of five hydrogen-loaded specimens. Stable crack growth region mostly consisted of transcrystalline cleavage fracture mechanism, **Figure 5**. Cracks also appeared abundantly on all test specimens, both in the initial region of the pre-cycled fatigue crack, **Figure 6a**), and in the region of stable growth, where they appeared to be coarser, **Figure 6b**).

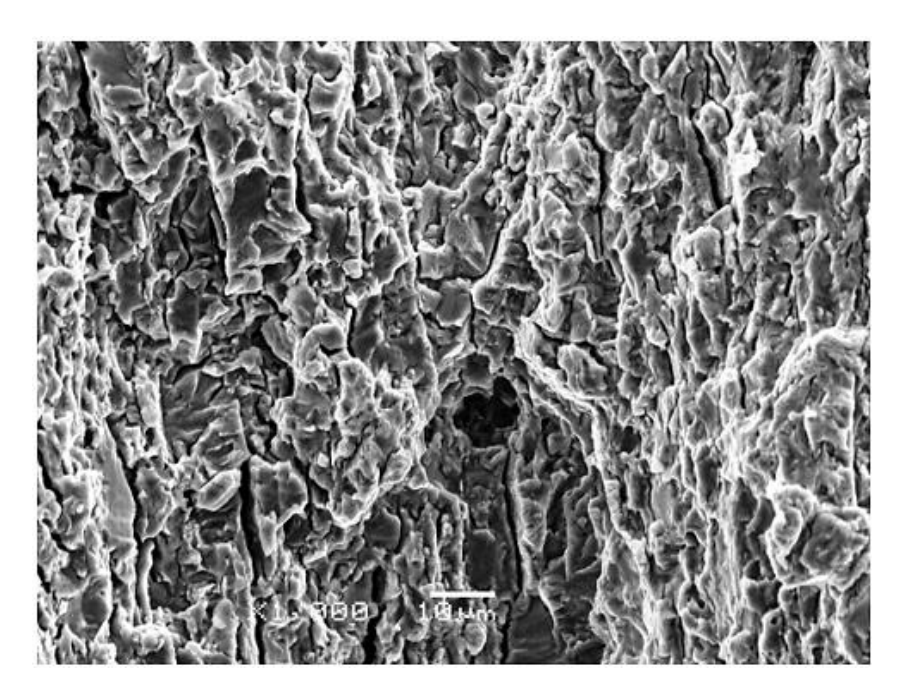


Figure 5 Transcrystalline cleavage fracture in stable crack growth increment in hydrogen-loaded specimen

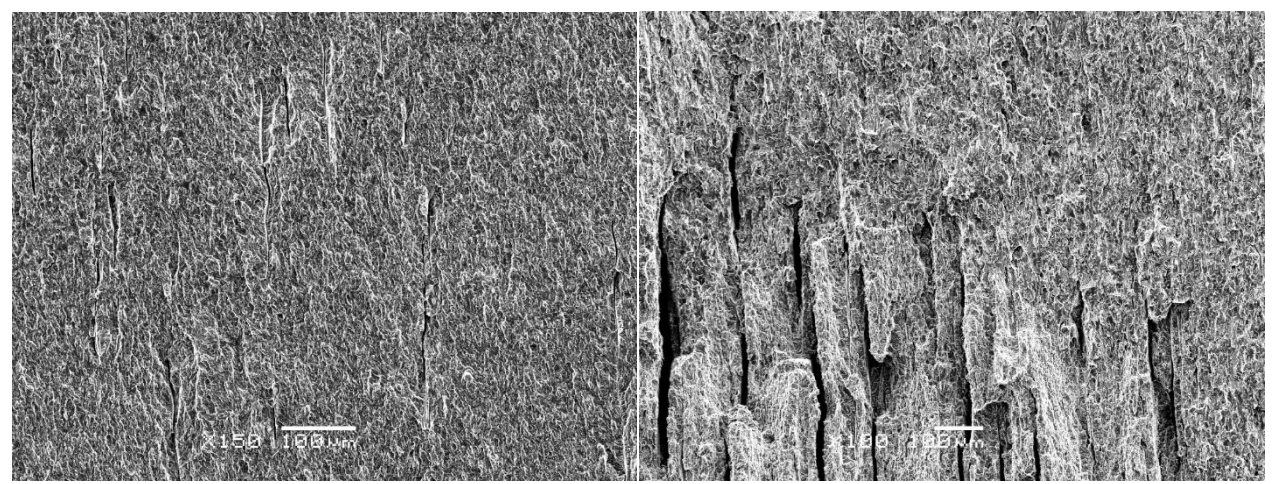


Figure 6a) Cracks in the initial region of the pre-cycled fatigue crack **6b)** cracks in the stable crack growth region

3. CONCLUSION

Based on above mentioned findings it can be stated that fracture toughness of the X-60 steel clearly decreased in hydrogen and is about 5 times lower in high-pressure hydrogen than in air. The decrease of fracture toughness is accompanied by change in fracture micromorphology from transcrystalline ductile dimple fracture in air to transcrystalline cleavage fracture in hydrogen, but no fisheyes were present which are a common fractographic sign in electrolytically charged specimen. Based on the fracture mechanism change the energy needed for fracture should be lower in high-pressure hydrogen but not as low as in electrolytically charged specimen because of the absence of the fisheyes.



ACKNOWLEDGEMENTS

This work was created as part of the TA CR project No. SS06020165 - Mapping the impacts of efforts to reduce greenhouse gas emissions using hydrogen additions on the lifetime of the existing infrastructure of gas power infrastructure plant and institutional support for the long-term and conceptual development of the research organization in 2025, which was provided by the Ministry of Industry and Trade of the Czech Republic.

REFERENCES

- [1] REPowerEU. Affordable, secure and sustainable energy for European Commission. [online]. 2022 [viewed: 2025-04-25]. Available from: https://commission.europa.eu/strategy-and-policy/priorities-2019-2024/european-green-deal/repowereu-affordable-secure-and-sustainable-energy-europe en
- [2] EHB Implementation Roadmap: Public support as catalyst for hydrogen infrastructure. European Hydrogen Backbone [online]. 2022 [viewed: 2025-04-25]. Available from: https://ehb.eu/page/publications
- [3] CRISTELLO, J.B., YANG, J.; HUGO, R., LEE, Y., PARK, S.S. Feasibility analysis of blending hydrogen into natural gas networks. *International Journal of Hydrogen Energy*. 2023, Vol. 48, No. 46, pp. 17605-17629. DOI: https://doi.org/10.1016/j.ii/hydene.2023.01.156.
- [4] LI, J., SU, Y., YU, B., WANG, P., SUN, D. Influences of Hydrogen Blending on the Joule–Thomson Coefficient of Natural Gas. *ACS Omega*. 2021, Vol. 6, No. 28, pp. 16722-16735. DOI: https://doi.org/10.1021/acsomega.1c00248.
- [5] FAYE, O., SZPUNAR, J., EDUOK, U. A critical review on the current technologies for the generation, storage, and transportation of hydrogen. *International Journal of Hydrogen Energy*. 2022, 47, pp. 13771-13802. DOI: <a href="https://doi.org/https://doi.org/https://doi.org/https://doi.org/https://doi.org/https://doi.org/https://doi.org/https://doi.org/https://doi.org/https://doi.org/https://doi.org/https://doi.org/https://doi.org/https://doi.org/https://doi.org/https://doi.org/https://doi.org/https://doi.org/https://doi.org/https://doi.org/https://doi.org/https://doi.org/https://doi.org/https://doi.org/https://doi.org/https://doi.org/https://doi.org/https://doi.org/https://doi.org/https://doi.org/https://doi.org/https://doi.org/https://doi.org/https://doi.org/https://doi.org/https://doi.org/https://doi.org/https://doi.org/https://doi.org/https://doi.org/https://doi.org/https://doi.org/https://doi.org/https://doi.org/https://doi.org/https://doi.org/https://doi.org/https://doi.org/https://doi.org/https://doi.org/https://doi.org/https://doi.org/https://doi.org/https://doi.org/https://doi.org/https://doi.org/https://doi.org/https://doi.org/https://doi.org/https://doi.org/https://doi.org/https://doi.org/https://doi.org/https://doi.org/https://doi.org/https://doi.org/https://doi.org/https://doi.org/https://doi.org/https://doi.org/https://doi.org/https://doi.org/https://doi.org/https://doi.org/https://doi.org/https://doi.org/https://doi.org/https://doi.org/https://doi.org/https://doi.org/https://doi.org/https://doi.org/https://doi.org/https://doi.org/https://doi.org/https://doi.org/https://doi.org/https://doi.org/https://doi.org/https://doi.org/https://doi.org/https://doi.org/https://doi.org/https://doi.org/https://doi.org/https://doi.org/https://doi.org/https://doi.org/https://doi.org/https://doi.org/https://doi.org/https://doi.org/https://doi.org/https://doi.org/https://doi.org/https://doi.org/https://doi.org/https://doi.org/https://doi.org/https://doi.org/https://doi.org/https://doi.org/https://doi.org/https://d
- [6] GasNet je připraven zvedat podíl biometanu a vodíku ve své síti [online]. 2022 [2025-04-25]. Available from: https://www.gasnet.cz/o-spolecnosti/novinky/2022/05/GasNet-je-pripraven-zvedat-podil-biometanu-a-vodiku
- [7] ISO 12135. Metallic materials *Unified method of test for the determination of quasistatic fracture toughness*. ISO. 2021.